CHAPTER III

Results

3.1 Giant tiger shrimp DNA extraction

Total DNA was extracted from the pleopods using a proteinase K-phenol-chloroform extraction procedure. From agarose gel electrophoresis as compared with standard DNA markers (λ/*Hind*III), the extracted DNA migrated as high molecular weight fragments of greater than 23.1 kb (Figure 3.1). The $OD_{260/280}$ ratio was higher than 1.8 indicating high purity. The DNA yield was about 15-30 μg/pleopod. The quality of obtained DNA was suitable for molecular procedures for the development of microsatellite DNA markers, e.g. restriction endonuclease digestion, cloning and being a template for PCR amplification in order to test the assessment of microsatellite alleles as described in Chapter II.

3.2 Preparation of restricted DNA fragments for cloning

For cloning, genomic DNA from one *P. monodon* (50 μg) was digested with a mixture of 4 restriction enzymes, including *Alu*I, *Hae*III, *Rsa*I, and *Hin*cII (25 units each), and 2 restriction enzymes, including *Alu*I and *Rsa*I (25 units each), all ot which produced blunt ended DNA fragments. The DNA fragments were separated on a 1.5% low melting agarose gel with a 100 bp size standard ladder (Figure 3.2). Genomic DNA fragments of 300-700 bp were recovered from the gel and the yield of recovery DNA was estimated to be 100 ng/μl using agarose gel electrophoresis as compared with standard DNA markers (λ/*Hind*III) (Figure 3.3).

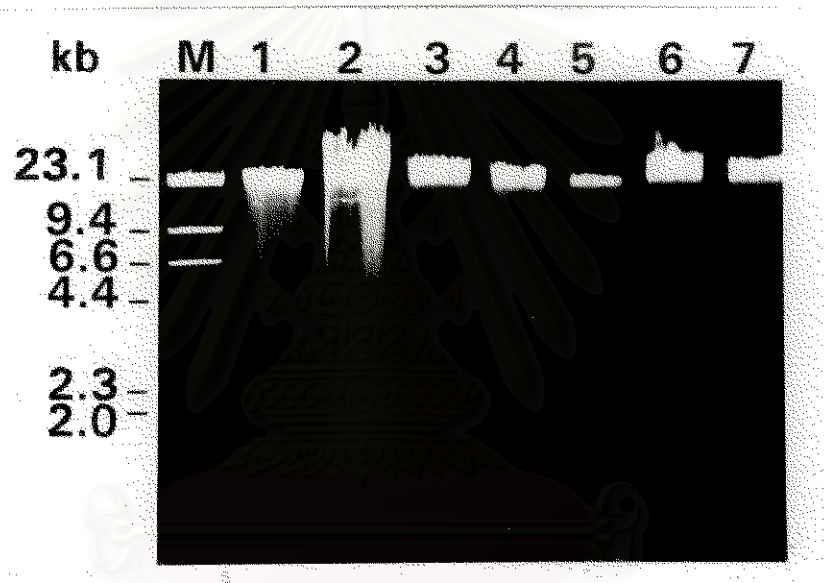

Figure 3.1 Ethidium bromide staining of extracted DNA from *P. monodon* pleopods. The DNA were subjected to electrophoresis on 0.8% agarose gel at 100 volts for 2 hours.

Lane M: DNA markers (λ/*Hin*dIII)

Lanes 1-7 : extracted shrimp DNA

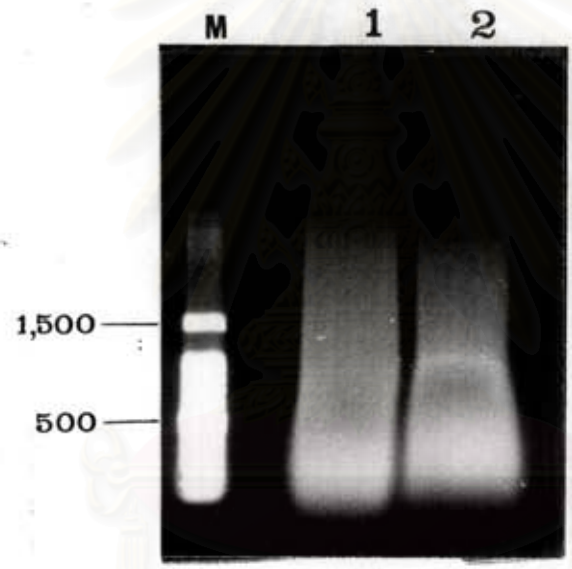

Figure 3.2 Ethidium bromide staining patterns of one individual *P. monodon* DNA separately digested with restriction enzymes. The DNA was subjected to electrophoresis on 1.5% agarose gel at 100 volts for 2 hours.

Lane M : DNA markers (100 bp ladder)

Lane 1 : shrimp DNA digested with *Alu*I, *Hae*III, *Rsa*I and *Hin*cII

Lane 2 : shrimp DNA digested with *Alu*I and *Rsa*I

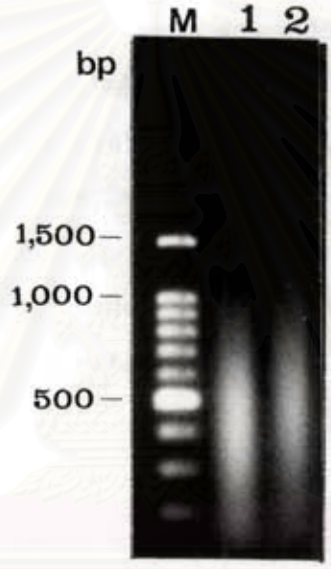

Figure 3.3 Ethidium bromide stainning of the recovered DNA fragments of 300-700 bp from low melting agarose gel. The DNA was run on 1.5% agarose gel at 100 volts for 2 hours.

Lane M : DNA markers (100 bp ladder).

Lane 1 : recovered DNA fragments of *P. monodon* DNA digested with of *Alu*I, *Hae*III, *Rsa*I and *Hin*cII

Lane 2 : recovered DNA fragments of *P. monodon* DNA digested with of *Alu*I and *Rsa*I.

3.3 Library construction and screening

3.3.1 Library A

The ligation mixture of 4 restriction enzyme digested DNA fragments of 300-700 bp were blunt-end ligated with *Sma*I-digested and phosphatased pUC18 DNA vector. Portions of the ligation mixture were transformed into *E. coli* DH5-α cells by both $CaCl_2$ and electroporation methods but the forrmer gave low number of transformants. The transformed cells were spread on LB agar plates contain 50 μl/ml ampicillin and screened for microsatellites by colony hybridization with ^{32}P end-labeled $(CT)_{15}$ and $(GT)_{15}$ oligonucleotide probes. A total of 60 positives clones (1.14%) from 5,250 transformant clones were obtained using $(CT)_{15}$ probe. An example of the results of colony hybridization was shown in Figure 3.4 a. When $(GT)_{15}$ probe was used, a total of 341 clones (3.22%) from 10,590 transformant clones were positive. An example of the results of colony hybridization was shown in Figure 3.5b.

3.3.2 Library B

For library B, DNA fragments prepared for ligation were obtained from 2 restrition enzyme digestion and host cells were changed to E. coli XL1-Blue cells. Transformants were selected with LB agar plates containg 12.5 μg/ml tetracyclin and screened for microsatellites by colony hybridization with a ^{32}P end-labeled $(GT)_{15}$ oligonucleotide probe. A total of 396 clones (7.92%) from 5,000 transformants were positive, Individual positive clones which gave strong hybridization signal were picked for DNA sequencing.

3.4 Characterization of microsatellites in *P. monodon*

3.4.1 Type of microsatellite arrays from library A.

Sixty of the 5,250 clones which were identified as putatively positive to a $(CT)_{15}$ probe were isolated and subjected to DNA sequencing. Sixty clones were sequenced and sixteen (26.7%) contain contained two or more microsatellite regions.

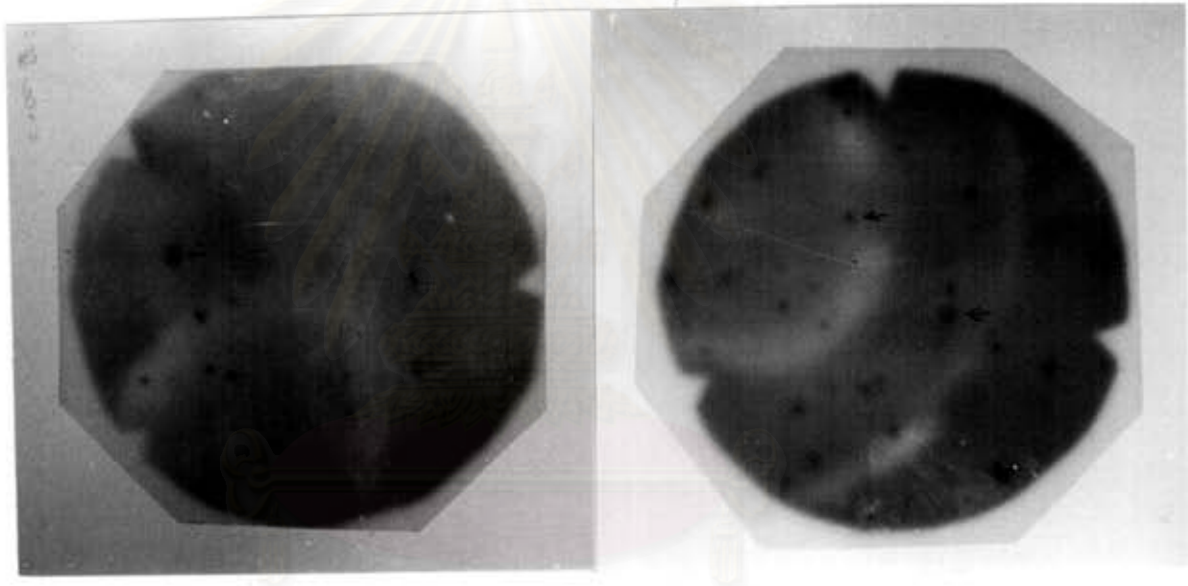

a. b.

Figure 3.4 Autoradiographs of colony hybridization screening for microsatellites from *P. monodon* genomic library A. Colonies which gave strong hybridization signal as indicated by the arrows were picked up for sequencing.

a. Screening with a ^{32}P labeled $(CT)_{15}$

b. Screening with a ^{32}P labeled $(GT)_{15}$

Although, the library was screened for $(CT/AG)_n$ microsatellites, several other microsatellite motifs were also obtained. A sequence was scored as a microsatellite when the numbers of repeats were $\geq$6 for dinucleotide repeats, $\geq$4 for trinucleotide repeats, and $\geq$3 for tetra, penta and hexanucleotide repeats (Stalling et al., 1991; Estoup et al., 1993). In this study, one clone contained tetranucleotide microsatellites, fitheen clones contained dinucleotide microsatellites.

Sixteen isolated microsatellite sequences were classified into three categories according to Weber (1990), namely, perfect, imperfect and compound repeats (Figure 3.5). Perfect repeats are uninterrupted stretches of the repeat units, while imperfect repeats contain one to three intervening bases within the stretches. Compound repeats have different motifs adjacent to each other. Examples of the sequences of perfect, imperfect and compound microsatellite repeats as shown in Figure 3.6. The types and repeat units were shown in Table 3.1-3.3. Most of the *P. monodon* microsatellites found in this study were imperfect repeats (12 loci, 75%, Table 3.2), two loci were perfect repeats (12.5%, Table 3.1) and two loci were compound repeats (12.5%, Table 3.3).

Table 3.1 Perfect microsatellites isolated from Library A using $(CT)_{15}$ as a probe.

Type	Characteristic of repeat unit	No. of clone
dinucleotide	$(AG)_n$	1
	$(CT)_n$	1

Table 3.2 Imperfect microsatellite isolated from Library A using $(CT)_{15}$as a probe.

Type	Characteristic of repeat unit	No. of clone
dinucleotide	$(AG)_n$	3
	$(CT)_n$	4
	$(GT)_n$	5

Table 3.3 Compound microsatellite isolated from Library A using $(CT)_{15}$as a probe.

Type	Characteristic of repeat unit	No. of clone
di-dinucleotide	$(CT)_{46}$ $(AT)_{42}$	1
di-tetranucleotide	$(CT)_{24}$ $(CCCT)_4$ CCACTC $(CT)_{32}$	1

Table 3.4 Perfect microsatellites isolated from Library A $(GT)_{15}$ as a probe.

Type	Characteristic of repeat unit	No. of clone
dinucleotide	$(CT)_n$	1
	$(AC)_n$	3
	$(AG)_n$	3
	$(GT)_n$	13

Table 3.5 Imperfect microsatellites isolated from Library A $(GT)_{11}$as a probe.

Type	Characteristic of repeat unit	No. of clone
dinucleotide	$(AT)_n$	2
	$(AC)_n$	3
	$(CT)_n$	1
	$(GT)_n$	11
di-dinucleotide	$(AC/AT)_n$	2
	$(AC/GT)_n$	1
	$(AT/GT)_n$	3
Di-trinucleotide	(GT/GGT)n	1
mixnucleotide	$(AC)_{34}$AAA $(AC)_{20}$ $(AT)_{26}$ $(ACT)_4$GTG $(ACT)_{21}$	1
	$(AC)_8$N $(AT)_{22}$ $(GT)_{14}$N $(CT)_{40}$	1

Table 3.6 Compound microsatellites isolated from Library A $(GT)_{16}$as a probe

Type	Characteristic of repeat unit	No. of loci
di-dinucleotide	$(AT)_{46}ATTA\ (AC)_{22}$	1
	$(GT)_9(AG)_{13}$	1
	$(AT)_6\ (GT)_{48}A\ (GT)_9A$	1
	$(CT)_{43}(AG)_{20}$	1
	$(GT)_{37}(AC)_9$	1
	$(AC)_{13}N\ (AC)_{12}$	1
	$(AT)_{29}(GT)_{41}$	1
	$(AC)_{16}ATCACAT(AC)_{25}$	1
	$(GT)_{47}AACA(AC)_6$	1
	$(AC)_{40}(AT)_{34}$	1
	$(AC)_8(GT)_{30}$	1
	$(GT)_{41}(CG)_6$	1
	$(AC)_6G(AC)_{46}(AT)44$	1
	$(AC)_{21}N(AC)_{39}(AT)_{42}$	1
	$(GT)_8N(GT)_{35}$	1
	$(GT)_6N(GT)_{47}TTAT(GT)_{21}$	1
	$(AC)_4(AT)_4$	1
	$(GT)_{33}N(GT)_6$	1
	$(AC)_{28}(AT)_{17}$	1
di-trinucleotide	$(TGA)_3GGA(TGG)_3CGGCGT(GA)_5$	1
	$(AC)_{34}AAA(AC)_{20}AT)_{26}(ACT)_4GTG\ (ACT)_{21}$	1
	$(GGT)_6(GT)_{26}(GT)_{40}$	1
tri-trinucleotide	$(TGT)_{10}TTTGCC(TGT)_{30}$	1
mixnucleotide	$(CT)_{28}(AT)_{22}(GT)_{80}$	1
	$(AC)_{21}(GT)_{24}(AC)_6$	1
	$(AC)_{44}N(AT)_{22}(AG)_{28}$	1
	$(AC)_8N(AT)_{32}(GT)_{14}N(CT)_{40}$	1
	$(AT)_{13}(AG)_8(GT)_{64}A(GT)_7A(GT)_{40}$	1

3.4.2 Type of microsatellite arrays from library B

Two hundred and twenty-five of the 6,390 clones which were identified as putatively positive to a $(GT)_{15}$ probe were isolated and subjected to DNA sequencing. Seventy-six clones (37.8%) were found to contain microsatellites. In this study, four clones contained trinucleotide microsatellites, sixty-seven clones contained dinucleotide microsatellites, and five clones contained mixed nucleotides as shown in Table 3.4-3.6. Of 76 loci, 20 loci (26.3%) were perfect repeats, 30 loci (39.5%) were imperfect repeats and 26 loci (34.2%) were compound repeats (Figure 3.7).

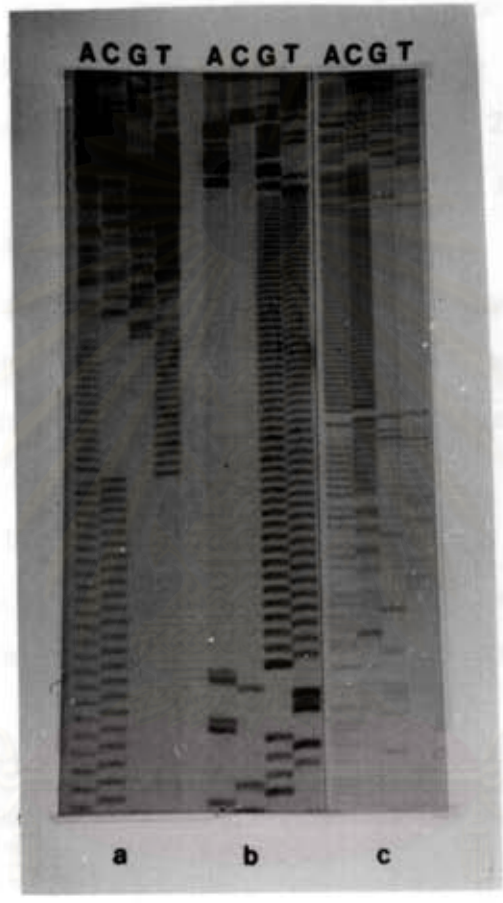

Figure 3.5 DNA sequences of perfect, imperfect and compound microsatellites

a. compound microsatellite

b. perfect microsatellite

c. imperfect microsqatellite

Two hundred and twenty-five of the 6,390 clones which were identified as putatively positive to a $(GT)_{15}$ probe were isolated and subjected to DNA sequencing. Seventy-six clones (37.8%) were found to contain microsatellites. In this study, four clones contained trinucleotide microsatellites, sixty-seven clones contained dinucleotide microsatellites, and five clones contained mixed nucleotides as shown in Table 3.4-3.6. Of 76 loci, 20 loci (26.3%) were perfect repeats, 30 loci (39.5%) were imperfect repeats and 26 loci (34.2%) were compound repeats (Figure 3.7).

One hundred and twenty one of the 2,400 clones which were identified as putatively positive to a $(GT)_{15}$ probe were isolated and subjected to DNA sequencing. Fourty clones were found to contain microsatellites. The library was screened for $(GT/AC)_n$ microsatellites, several other microsatellite motifs were shown (Table 3.7 to 3.9).

Of 40 loci, 11 loci (27.5%) were perfect repeats, 17 loci (42.5%) were imperfect repeaats and 12 loci (30.0%) were compound repeats (Figure 3.8).

Table 3.7 Perfect microsatellites isolated from Library B Using $(GT)_{15}$as a probe.

Type	Characteristic of repeat unit	No. of clone
dinucleotide	$(AT)_n$	1
	$(AC)_n$	3
	$(GT)_n$	7

Table 3.8 Imperfect microsatellites isolated from Library B Using $(GT)_{15}$as a probe.

Type	Characteristic	No. of clone
mono-nucleotide	$(A)_n$	1
	$(T)_n$	1
mono-manonucleotide	$(A/G)_n$	1
dinucleotide	$(CT)_n$	1
	$(AC)_n$	2
	$(GT)_n$	6
	$(AT)_n$	3
di-dinucleotide	$(AC/GT)_n$	1
di-trinucleotide	$(AGT)_n$ $(GT)_n$	1

Table 3.9 Compound microsatellites isolated from Library B Using $(GT)_{15}$as a probe.

Type	Characteristic	No. of clone
mono-monodinucleotide	$(T)_{11}(A)_{14}$	1
	$(AC)_{20}(A)_{27}$	1
di-dinucleotide	$(AT)_{16}(GT)_{62}$	1
	$(AT)_{20}(GT)_{57}$	1
	$(GT)_{14}(CT)_{9}$	1
	$(AT)_{12}(GT)_{60}$	1
	$(AT)_{20}(GT)_{15}(AT)_{13}$	1
di-trinucleotide	$(AC)_{6}(TAC)_{7}$	1
di-hexanucleotide	$(GTGTGC)_{4}(GT)_{61}$	1
mixeddinucleotide	$(GT)_{83}[CT(GT)_{5}]_{9}$	1
momo-di-tetranucleotide	$(GT)_{19}N_{4}(GT)_{14}(CCGT)_{4}$	1
di-tetra-hexanucleotide	$(GT)_{34}A(AGTGTG)_{6}(AGTG)_{32}$	1

3.4.3 Distribution of microsatellite sequences

3.4.3.1 Distribution of $(CT/AG)_n$ sequence

From library A, a total of 16 $(CT/AG)_n$ microsatellite arrays were identified. A rough estimate of the average distance between arrays $(CT/AG)_n$ arrays occurring in the genome was calculated. The partial genomic library of approximately 5,250 clones containing an average insert size of 500 bps was constructed, representing 5,250 x 500 = 2,625 x 10^6 bp of giant tiger prawn genomic DNA. The crude average distance between neighboring microsatellites can be estimated by dividing the total length of screened DNA by the number of isolated microsatellites. Thus, in the cloned fraction of the giant tiger prawn genome, (GT/AG)n microsatellites occurred on an average of every 164 kb. The average distances of (GT/AG)n microsatellite in the genomes of various invertebrate species, fish and mammals were compared with that of giant tiger shrimp as shown in Table 3.10.

3.4.3.2 Distribution of (GT/CA)n sequence

A total of 76 $(GT/AC)_n$ microsatellite arrays were identified from the partial genomic library of approximately 6,390 clones containing an average insert size of 500 bp, representing 6,390 x 500 = 3.195 x 10^6 bp of giant tiger shrimp genomic DNA. Thus, in the cloned fraction of the giant tiger prawn genome, $(GT/AC)_n$ microsatellites occurred on an average of every 42 kb. The average distances of $(GT/AC)_n$ microsatellites in the genomes of various invertebrate species, fish and mammals were compared with that of giant tiger prawn as shown in Table 3.10.

3.4.4 Repeat lengths

3.4.4.1 Library A

The longest perfect stretches of $(CT/AG)_n$ microsatellite arrays which were identified from the sixteen clones were plotted according to classes and numbers of uninterrupted repeat units as shown in Figure 3.6. The number of $(CT/AG)_n$ repeats ranged from 6 to more than 48 repeat units. Most of the arrays of $(CT/AG)_n$ were imperfect motifs. The most common size class for $(CT/AG)_n$ microsatellites isolated from library A was 12-17 repeats.

The longest perfect stretches of $(GT/AC)_n$ microsatellite arrays which were identified from the library A and B were plotted according to classes and numbers of uninterrupted repeat units as shown in Figure 3.7 and 3.8. The number of $(GT/AC)_n$ repeats ranged from 6 to more than 96 bp in library A and 6 to more than 85 bp in library B. Most of the arrays of $(GT/AC)_n$ were imperfect motifs which made up 39.5% of a total of 30 loci and 42.5% of a total of loci. The most common size class for $(GT/AC)_n$ microsatellites isolated from library A and B were 36-45 and 46-55 repeats.

Proportion of each category, the most common category classes, and the longest size categories for $(CT)_n$ and $(GT)_n$ microsatellites in giant tiger prawn were compared with microsatellites from other species : honey bee (Estoup et al., 1993), human (Weber, 1990), pig (Wintero et al., 1992), Atlantic salmon (Slettan et al., 1993), rainbow trout (Morris et al., 1996) and Atlantic cod (Brooker et al., 1994) as shown in Table 3.11.

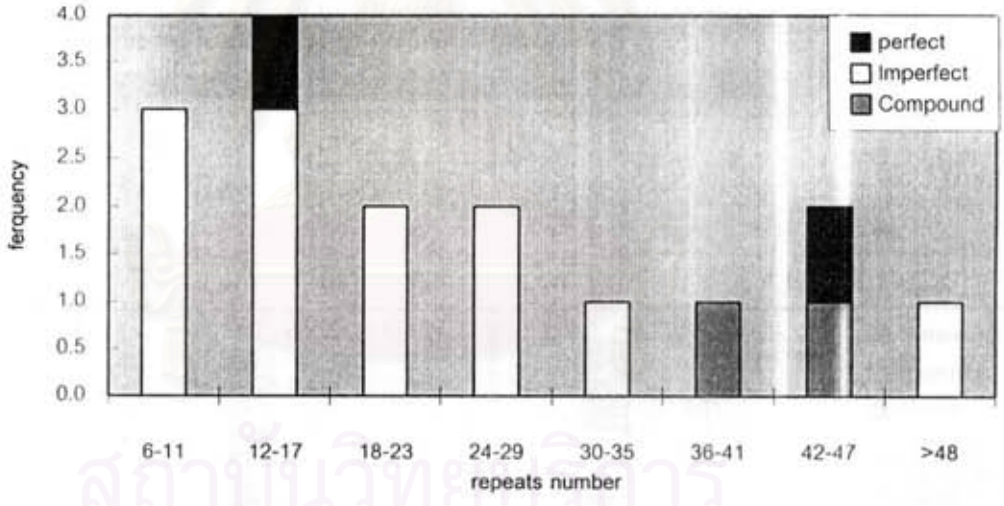

Figure 3.6 Frequency of different size classes of the longest uninterrupted (CT/AG)n microsatellite arrays from *P. monodon* from library A. Size classes are represented as number of repeat units.

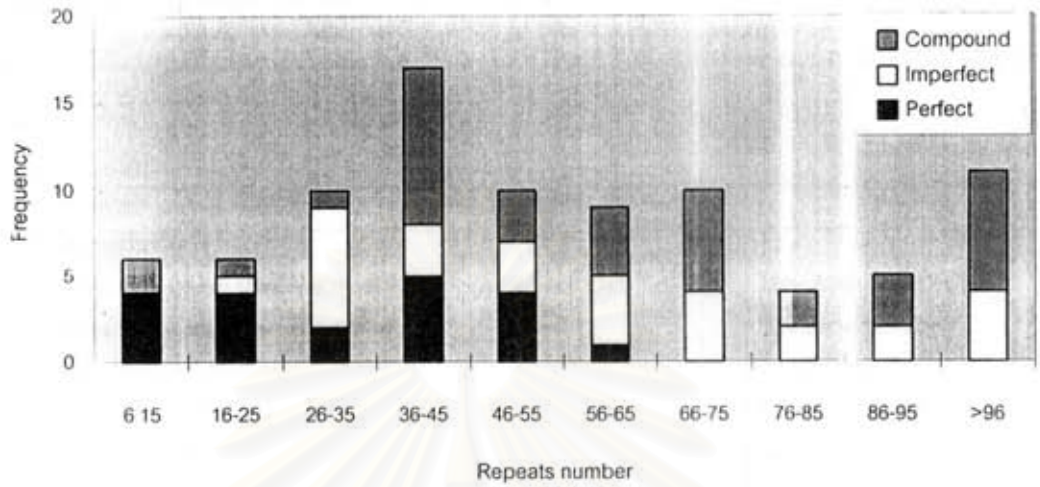

Figure 3.7 Frequency of different size classes of the longest uninterrupted (GT/AC)n microsatellite arrays from *P. monodon* from library A. Size classes are represented as number of repeat units.

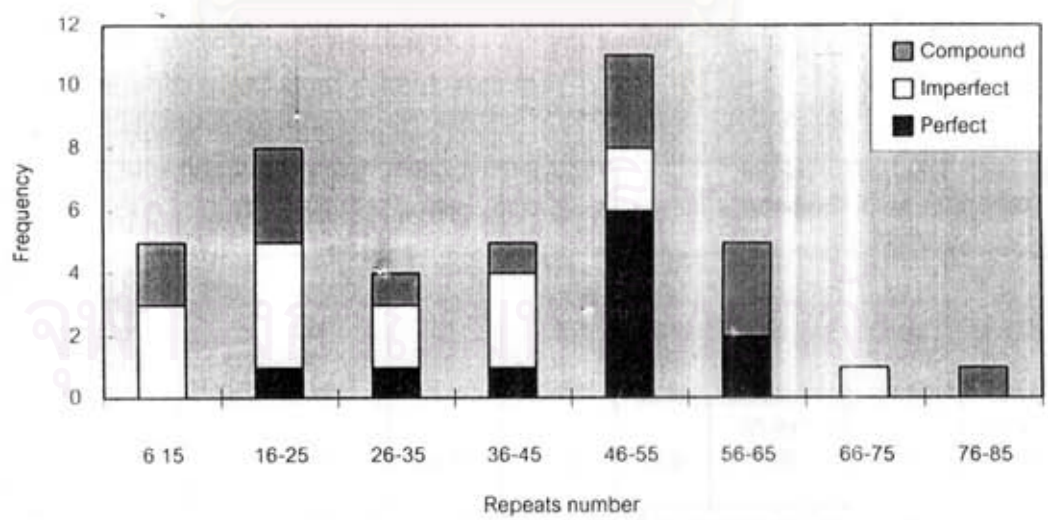

Figure 3.8 Frequency of different size classses of the longest uninterrupted (GT/AC)n microsatellite arrays from *P. monodon* from library B. Size classes are represented as number of repeat units.

Table 3.10 Average distance in kb between $(CT)_n$ or $(GT)_n$ microsatellites in genome of invertebrate, various fish and mammal species compared to giant tiger prawn.

Species	Average distance (kb)	Source
Invertebrates		
Giant tiger prawn (*Penaeus monodon*)	92.8 of $(GT)_n$	Mrs. Amornrat' Thesis
Giant tiger prawn (*Penaeus monodon*)	164 $(CT)_n$	The present study
Giant tiger prawn (*Penaeus monodon*)	42 of $(GT)_n$	The present study
Honey bee (Apis mellifera)	34 of $(GT)_n$	Estoup et al., 1993
European flat oyster (Ostrea edulis)	139 of $(GT)_n$	Baciri et al., 1995
Fish		
Atlantic cod (Gadus morhua)	7 of $(GT)_n$	Brooker et al., 1994
Atlantic salmon (Salmo salar)	90 of $(GT)_n$	Slettan et al., 1993
Brown trout (Salmo trutta)	23 of $(GT)_n$	Moriss et al., 1996
Mammals		
Human (Homo sapiens)	28 of $(GT)_n$	Weber, 1990
Porcine (Sus sp.)	46 of $(GT)_n$	Wintero et al., 1992

Table 3.11 Percentage of different categories and sizes of $(GT)_n$ microsatellites in honey bee, human, pig, Atlantic salmon, rainbow trout and Atlantic cod compared with giant tiger prawn genome.

	Giant tiger prawn		**Honey bee**	**Human**	**Pig**	**Atlantic salmon**	**Rainbow trout**	**Atlantic cod**
	(1)	**(2)**						
n	16	76	23	114	105	45	51	64
% perfect	12.5	26.3	48	64	71	80	56.9	48.4
% imperfect	75	39.5	22	25	19	20	31.4	45.3
% compound	12.5	34.2	10	11	10	0	11.7	6.3
Most common size class	12-17	36-45	7-9	12-15	16-18	6-9 (21-24)*	24-29	6-11 (30-35)*
Largest size class	>48	>96	85-87	27-30	28-30	>33	>60	>60

The crifterion which define an imperfect repeat were altered to incorporate four or five intervening bases rather than three.

(1) $(CT)_n$ microsatellite probe

(2) $(GT)_n$ microsatellite probe

3.5 Polymorphism of microsatellites in *P. monodon*

PCR primers were designed from the unique flanking sequences of 3 microsatellites loci from library A; Pmo 131, Pmo 142, Pmo 195 and from library B, Pmo 517, Pmo 519, Pmo 524. Primers for amplification of microsatellite loci by PCR were shown in Table 3.12 and 3.13. Although partial or complete sequence data were obtained from 132 microsatellite clones, several of them (more than 90%) had at least one cloning site located adjacent to or very close to the microsatellite sequence, thus preventing the design of primer from unique flanking sequences. Most of the flanking regions of microsatellites in clones that contained 2 or more microsatellites regions were too short to be used for primer design. Some microsatellites were flanked by sequences consisting mainly of the same bases contained in the microsatellite, making the primer design difficult.

From 3 primer sets tested, 2 primer sets namely Pmo131, Pmo195 from library A produced fragments whose sizes were as expected whereas the others gave nonspecific amplifications. Only 1 of 3 microsatellite primer sets from library B, namely, Pmo 519 produced fragments whose sizes were as expected. The PCR conditions for each primer set such as annealing temperatures, ratios of unlabeled to radioactive labeled primer and magnesium concentrations were optimized as shown in Table 3.12, 3.13.

Pmo 131 locus

This locus contained trinucleotide repeats, $(GTT)_{17}$. The nucleotide sequences of the microsatellite clone and the primers designed from the flanking regions were shown in Figure 3.9. The initial annealing temperatures for Pmo 131 locus were estimated to be 53°C and 51°C for forward and reverse primers, respectively. PCR amplifications of Pmo 131 locus were performed at 51°C, under the standard PCR conditions for both labeled primers. Nonspecific amplification

Table 3.12 Nucleotide sequences of *P. monodon* microsatellite primers amplification of loci by PCR from library A

Locus	Repeat units	5'-3' Primer	Annealing temperature (°C)	Expected size (bp)
Pmo 131	(GTT)17	f TGTAGTAGACTGATGATGCG	51	72
		r GATAGACCCAATAAGACAGA		
Pmo 142	$(GT)_{18}$	f ACGGAAAGTCATTGTTTGC	49	87
		r AAGACAGAATCCCAAGTCG		
Pmo 195	$(GT)_{36}$	f CAAACACTATCTCGCATTCT	51	112
		r CTCTATCCTCACACTGCTAA		

f = forward primer

r = reverse primer

Table 3.13 Nucleotide sequences of *P. monodon* microsatellite primers for amplification of loci by PCR from library B

Locus	Repeat units	5'-3' Primer	Annealing temperature (°C)	Expected size (bp)
Pmo 517	$(GT)_{62}$	f GATAGGTTGTACTCACAT	56	172
		r ACAGGCAACGCAAGCAGC		
Pmo 519	$(GT)_{40}$	f CAGACATGAACCTACCGTTA	56	166
		r CGAGCTGCATGTAACGTATA		
Pmo 524	$(GT)_{66}$	f CAGGCCTCGCTATCCTACC	53	185
		r AGCAGCATTGACATGATACG		

f = forward primer

r = reverse primer

fragments were detected from 6 unrelated individual templates as shown in Figure 3.10. Optimization of PCR conditions were carried out to get rid of the nonspecific products by decreasing the annealing temperature to 50°C but the expected fragments were not amplified. A touch down PCR temperature profile was also used for amplification at the Pmo131 locus, however, at annealing temperature of 52°C and 50°C, the amplification patterns obtained were not scorable (Figure 3.11 a, 3.11 b).

5′

TAC AGC TAT TCT TAT CGA GCG AAA TGT CAT TGT TTG ACT ATG TGT

AGT AGA CTG ATG ATG CG GAT GAT $(GTT)_{17}$GAT AGA TGA CAC TGA TAA

3′

CCT ATC TGG GTT ATT CTG TCT TAA CGT TCA GGT GTT ATA CTG TGT

Figure 3.9 The nucleotide sequences of the microsatellite clone, Pmo 131 locus and the position of primers designed from the flanking regions (under lined).

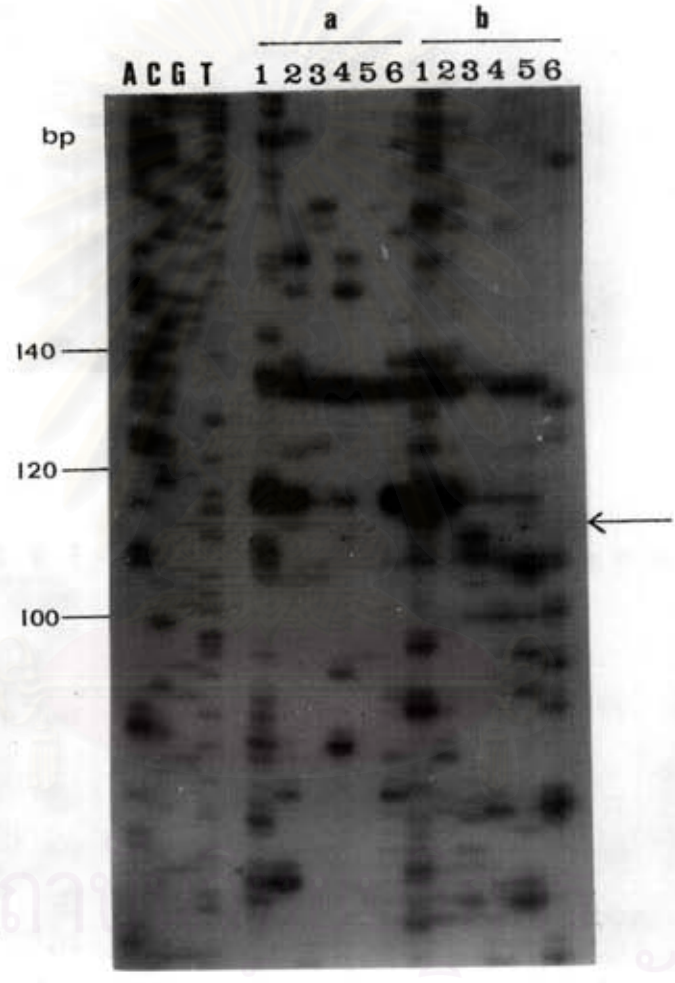

Figure 3.10 PCR amplification patterns of Pmo 131 locus from six unrelated individual *P. monodon* DNA at 51°C. Annealing temperature under the standard PCR conditions was 51°C. The M13 sequencing ladder was used as standard size marker.

a. ^{32}P-labeled forward primer

b. ^{32}P-labeled reverse primer

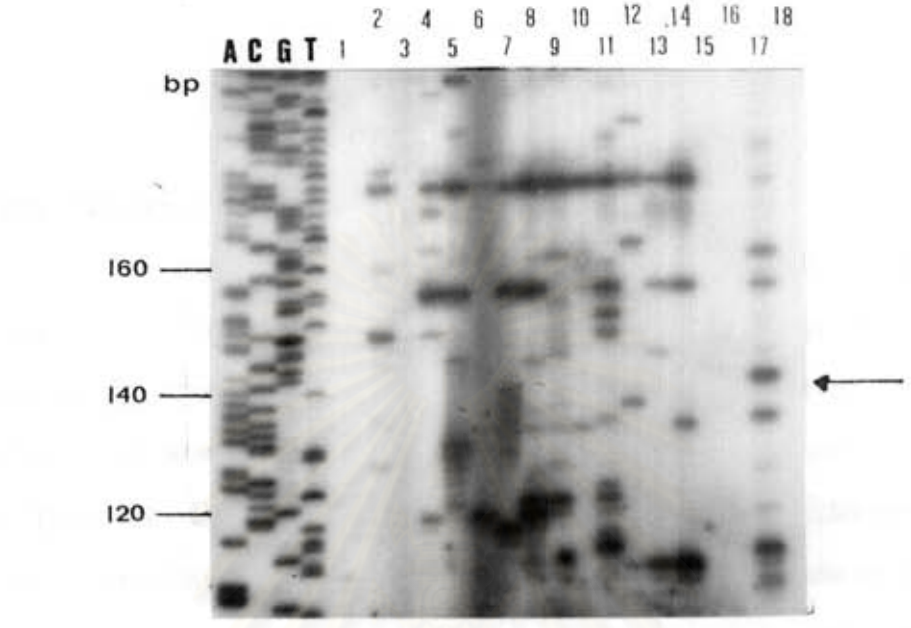

a.

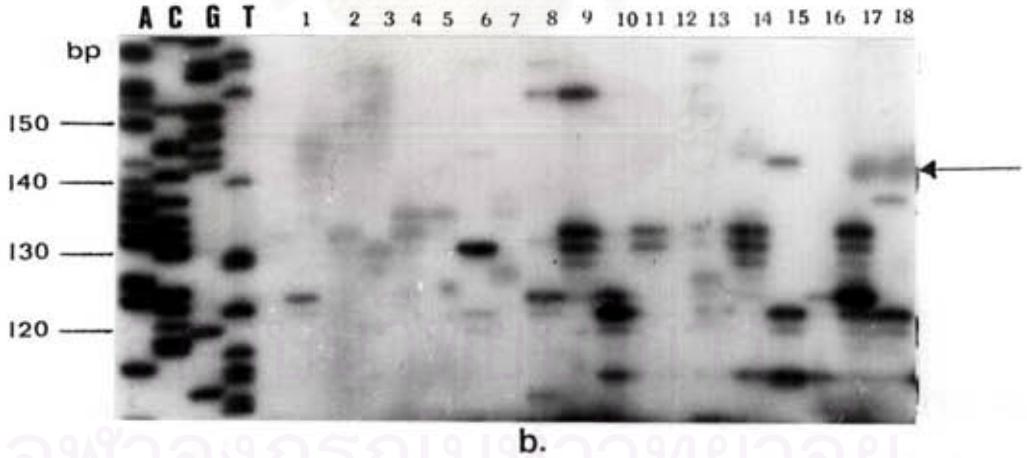

b.

Figure 3.11 PCR amplification patterns of Pmo 131 locus from eighteen unrelated individual *P. monodon* DNA. Forward primer was ^{32}P-labeled and the arrow indicated stutter microsatellite alleles. The M13 sequencing ladder was used as standard size marker.

a. Using the touch down PCR conditions at 52°C

b. Using the touch down PCR conditions at 50°C

Pmo 142 locus

This locus contained dinucleotide repeats, $(GT)_{18}$. The nucleotide sequences of the microsatellite clone and the primers designed from the flanking regions are shown in Figure 3.12. The annealing temperature for Pmo 142 locus were estimated to be 49°C and 51°C for forward and reverse primers, respectively. PCR amplifications of Pmo 142 locus were performed at 2 different annealing temperatures, 49°C and 51°C, under the conditions for both ^{32}P-labeled primers. Nonspecific amplification fragment were detected from 12 unrelated individual templates. Although the annealing temperature was decreased, nonspecific products were still observed and alleles could not be scrored as shown in Figure 3.13.

5′

ACG TAT CTA CTG ACG GAA AGT GAT CAT TGT TTG CA ATC TTG ATG AGT GGA CGT AGT AGT CGG A $(TG)_{18}$ AGA TGA AAG TAC GAC TGT GGA

3′

CG CGA CTT GGG ATT CTG TCT T AA TGA CCA GGT GTT

Figure 3.12 The nucleotide sequences of the microsatellite clone, Pmo 142 locus and the primers designed from the flanking regions (under lined).

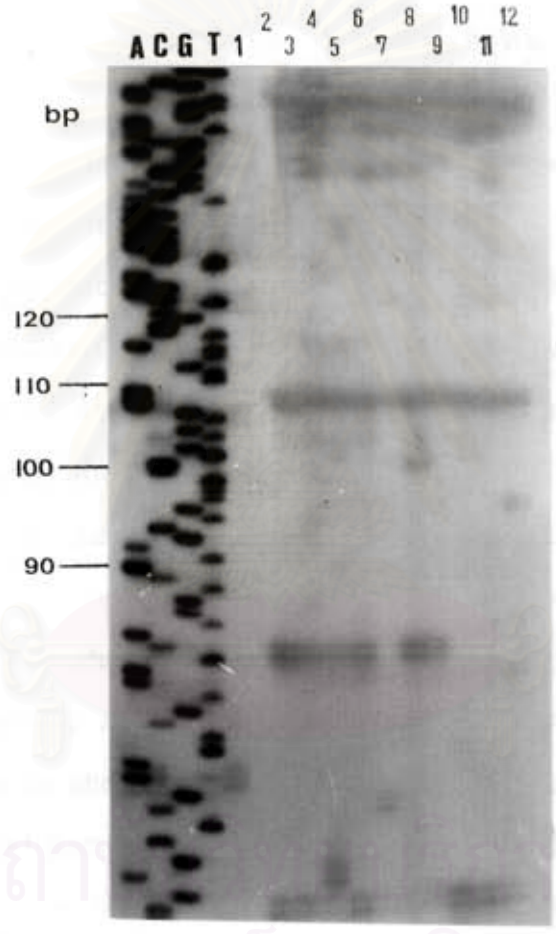

Figure 3.13 PCR amplification patterns of Pmo 142 locus from twelve unrelated individual P. monodon DNA at 49°C for the initial annealing temperature under the standard PCR conditions by using ^{32}P-labeled reverse primer. M13 sequencing ladder was used as standard size marker.

Pmo 195 locus

The Pmo195 locus consisted of $(GT)_{38}$ repeats. The nucleotide sequences of the clone and primers designed from the flanking regions are shown in Figure 3.14. PCR amplifications of Pmo 195 locus were performed at the initial annealing temperature of 51°C and 53°C for ^{32}P-labeled forward and reverse primers, respectively, under the standard PCR condition.. The results showed intense nonspecific products but faint stutter bands which were the indication of microsatellite alleles appeared (Figure 3.15a, b). The alleles from PCR amplifications were not scorable because of the interference from nonspecific amplification products. Optimization of PCR conditions were done in order to get the scorable products by changing the annealing temperatures, the concentration of $MgCl_2$, decreasing the concentration of primers and Tween 20 as summerized in Table 3.14. At the final optimized conditions, the stutter bands of PCR amplifications were scorable but nonspecific amplification fragments were still strongly detected as shown in Figure 3.16. The PCR patterns of 24 unrelated individual *P. monodon* showed polymorphic fragments which were scored for the allelic genotypes as shown in Table 3.15. It was found that 15 alleles were ambigously scored from a total of 48 possible alleles. Four individual (128/128, 123/109, 126/119, 124/98) were heterozygous. The sizes of the observed alleles ranged from 97 to 128 bp. Homozygosity of Pmo195 45.8% and heterozygosity 20.8%

5′

GAT AGG AGT CGG ACA GAC GAA CGG CAA ACA CTA TCT CGC ATT CT

TCC CA $(TG)_{36}$ TAA CGA ACA TGC ACT ACC TTA CGA GTG TGA GG

3′

A TAG AG T AAG AGC AGG TAT ACT GTC CTA CAG TGA AGA AG

Figure 3.14 The nucleotide sequences of the microsatellite clone, Pmo 195 locus and the primers designed from the flanking regions (underlined).

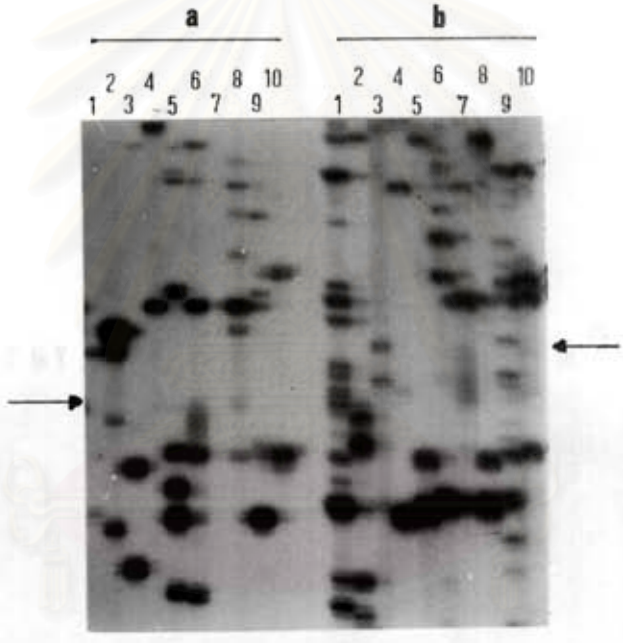

Figure 3.15 PCR amplification patterns of Pmo 195 locus from 10 unrelated individual P. monodon DNA 51°C annealing temperature under the standard PCR conditions. Arrows indicated microsatellite alleles.

a. ^{32}P-labeled forward primer

b. ^{32}P-labeled reverse primer

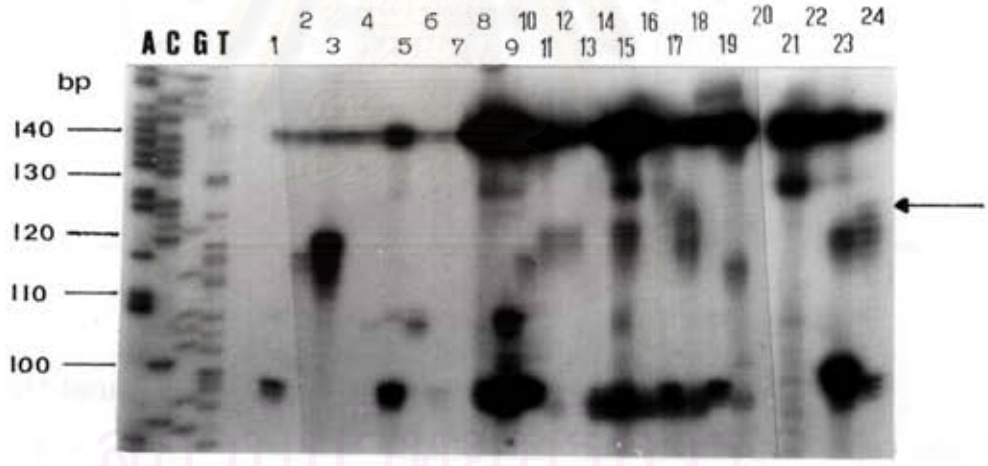

Figure 3.16 PCR amplification patterns of Pmo 195 locus from 24 unrelated individual P. monodon DNA (lane 1-24) at 51°C annealing temperature under the standard PCR conditions. The M13 sequencing ladder was used as stardard size marker.

Table 3.14 Optimization of PCR conditions for Pmo 195 locus

Trial No.	Labeled primer	PCR conditions	Results	Description
1.	F R	Ta = 51°C Ta = 53°C	PCR amplification of labeled forward primer gave better result.	Figure 3.15
2.	F	At 51°C the concentration of $MgCl_2$ (a) decreased to 7.5 and 5 mM (b) increase to 15 and 20 mM	At 15 mM of MgCl2, the results were the best. (The standard MgCl2 concentration in PCR amplification was 10 mM)	Data not shown
3.	F	Ta = 53°C with 15 mM MgCl2	The result was worse than that of standard condition in figure 3.15	Data not shown
4.	F	Ta = 51°C with 15 mM MgCl2 and without Tween 20	The result was worse than that ofstandard condition in figure 3.16	Data not shown
5.	F	Ta = 51°C and adjust the unlabeled forward primer concentration (F:R) to the ratio of 1:2, 1:4 and 1:8 with 15 mM MgCl2	With the ratio of 1:2 (F:R), the results were better	Figure 3.16

Pmo 517 locus

This locus contained dinucleotide repeats,$(GT)_{53}$. The nucleotide sequences of the microsatellite clone and the primers designed from the flanking regions are shown in Figure 3.17. The initial annealing temperature for Pmo 517 locus were estimated to be 51°C and 53°C for forward and reverse primers, respectively. PCR amplifications of Pmo 517 locus were performed at two different annealing temperatures, 51°C and 53°C, under the standard PCR conditions for both labeled primers. The results in Figure 3.18 revealed intense bands of PCR amplification products, but the alleles from PCR amplifications of the labeled reverse primer had more nonspecefic amplification products than did

forward primer. Optimization of PCR conditions were done in order to get the scorable products by changing the annealing temperatures and the concentration of $MgCl_2$ but the nonspecific amplification fragments were still detected while expected fragments were not amplified as shown in Figure 3.19.

Table 3.15 Microsatellite variation of Pmo195 locus in 24 unrelated individual prawns

Individual prawn	Genotype*
1	98/98
2	118/118
3	121/121
4	no amplification product
5	98/98
6	108/108
7	97/97
8	no amplification product
9	128/128
10	107/101
11	118/118
12	121/121
13	121/121
14	no amplification product
15	123/109
16	no amplification product
17	126/119
18	no amplification product
19	117/117
20	no amplification product
21	no amplification product
22	no amplification product
23	122/100
24	124/98

* Genotype were scored from the amplification pattern in Figure 3.16

5′

TCG ATA GGT TGT ACT CAC AT GTGC ATA CAC ATA TTG CAA CAT TGT AAT GCA

GAG CGT GTG AAT TTC AA $(GT)_{53}$ TT GAG AT GG AGA AAG AGA GTG GTG AGT

GAG ATG CGC GCT GTT TTA $G(T)_6$ GCA TGC T GC TGC TTG CGT TGC CTG T CT TAG

3′

CCT TGA

Figure 3.17 The nucleotide sequences of the microsatellite clone, Pmo 517 locus and the primers designed from the flanking regions (under lined).

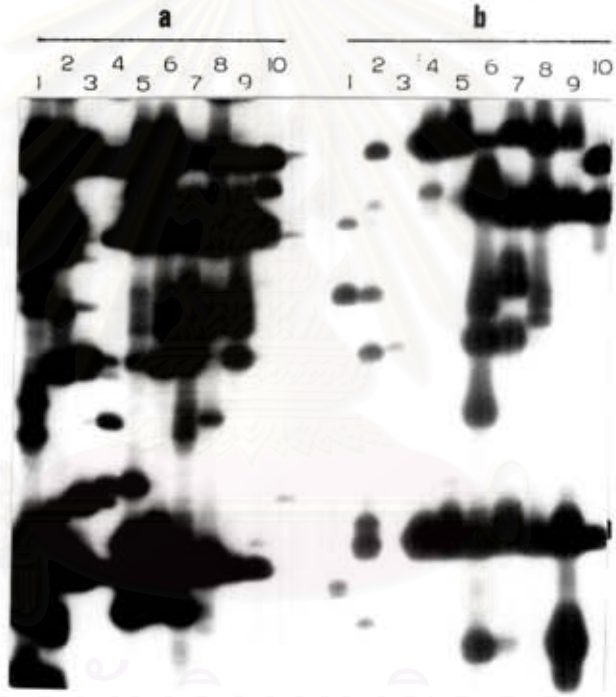

Figure 3.18 PCR amplification patterns of Pmo 517 locus from 10 unrelated individual P. monodon DNA at 51°C for the initial annealing temperature under the standard PCR conditions.

a. ^{32}P-labeled Reverse primer

b. ^{32}P-labeled Forward primer

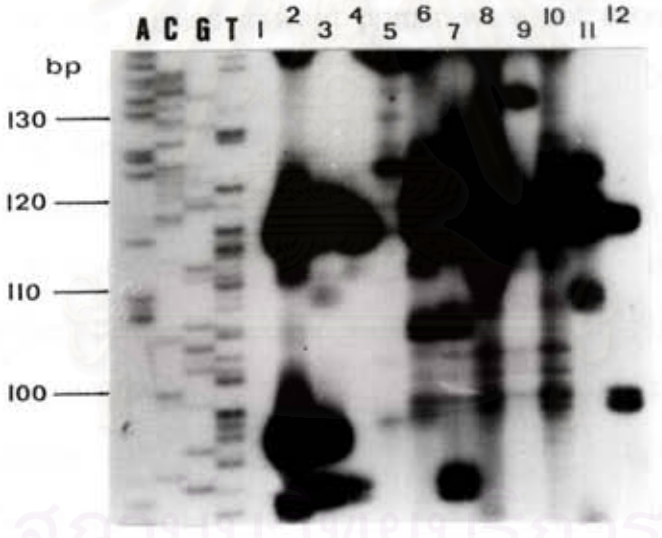

Figure 3.19 PCR amplification patterns of Pmo 517 locus from 12 unrelated individual P. monodon DNA by using ^{32}P-labeled forward primer at 51°C annealing temperature under the standard PCR conditions. The M13 sequencing ladder was used as standard size marker.

Pmo 519 locus

The locus contained dinucleotide repeats, $(GT)_{53}$. The nucleotide sequences of the microsatellite clone and the primers designed from the flanking regions are shown in Figure 3.20. The annealing temperature for Pmo 519 locus was estimated to be 53°C for reverse and forward primers, respectively. PCR amplifications of Pmo 519 locus were performed at annealing temperature of 53°C the standard PCR conditions for both labeled primers. The results in Figure 3.21 revealed intense bands of PCR amplification products with stutter bands of microsatellite alleles. The alleles from PCR amplifications of the labeled reverse primer were not amplification patterns obtained. However, the alleles from PCR amplifications of the labeled forward primer were not scorable because of the interference from nonspecific amplification products. Optimization of PCR conditions were done in order to get the scorable products by changing the annealing temperatures, the concentration of Tween 20 as summerized in Table 3.16. At the final oplimization conditions, the microsatellite alleles at Pmo519 were amplifiable and showed polymorphic PCR products (Figure. 3.22). However, nonspecific products were still strongly amplified and interfered with the microsatellite score. Allelic genotypes from 10 unrelated individual *P. monodon* were scored from the PCR patterns in Figure 3.22. It was found that 9 alleles were not unambigously scored from a total of 20 possible alleles. Three individuals (136/129, 131/115, 133/111) were heterozygous. The sizes of 10 observed alleles ranged from 111 to 138 bp. The sizes of the first band of each allele which were obtained from the PCR amplifications were determined using the M13 sequencing markers as shown in Table 3.17. Homozygosity of Pmo 519 30.0% and heterozygosity 40.0%.

5′

ACC ACG GCAG GCT CAG ACA TGA ACC TAC CGT TAA AAG AAG AA

AGA AGA $(GT)_{40}$ CGT TCG GTC TGG CAT ATG TGG CTG CGG GG

3′

ATC CGA GCT CGA CGT ACA TTG CAT ATG CTG TGT TC

Figure 3.20 The nucleotide sequences of the microsatellite clone, Pmo519 locus and the primers designed from the flanking regions (under lined).

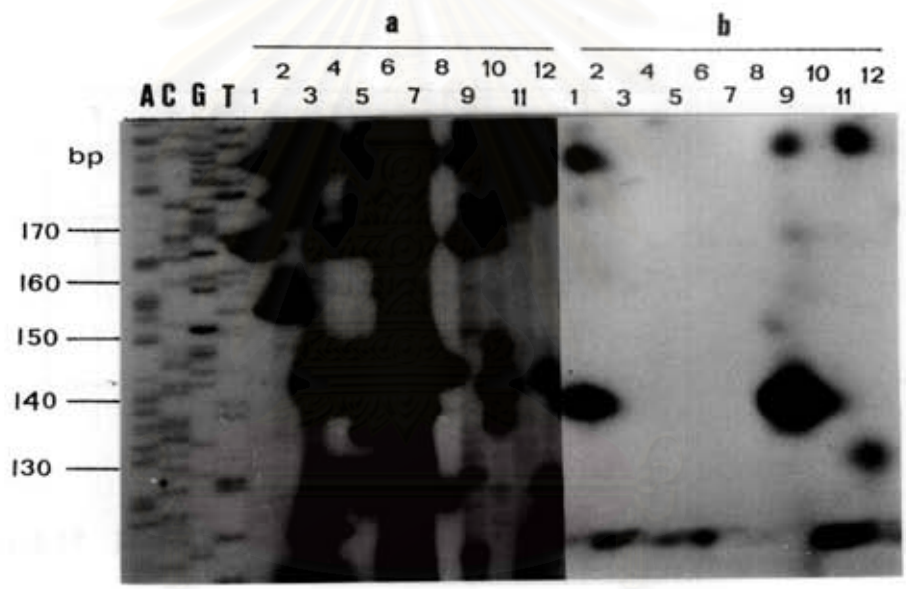

Figure 3.21 PCR amplification patterns of Pmo 519 locus from 12 unrelated individual P. monodon DNA at 53°C annealing temperature under the standard PCR conditions. The M13 sequencing ladder was used as standard size marker.

a. ^{32}P-labeled forward primer

b. ^{32}P-labeled reverse primer

Table 3.16 Optimization of PCR conditions for Pmo 519 locus

Trial No.	Labeled primer	PCR condition	Results	Descrip-tion
1.	F	Ta = 53°C	PCR amplification of labeled forward primer gave better result.	Figure 3.21
	R	Ta = 53°C		
2.	F	At 53°C, the concentration of $MgCl_2$ was (a) decreased to 5 and 7.5 mM (b) increased to 15 and 20 mM	The standard $MgCl_2$ concentration (10 mM) in PCR provided the best result of PCR amplification.	Data not shown
3.	F	Ta = 55°C with 0.05% of Tween 20	The best PCR amplifications were at 56°C and 0.05% Tween 20	Figure 3.22
4.	F	Ta = 55°C and adjust the concentration of unlabeled forward primer to unlabeled reverse primer (F:R) to the ratio of 1:2 and 1:4	The best PCR was amplifiable at standard primer concentration 0.6 μM.	Data not shown

Table 3.17 Microsatellite variation of Pmo 519 locus in 10 unrelated individual prawns.

Individual	Genotype
1	139/129
2	134/134
3	128/128
4	no amplification product
5	131/116
6	127/127
7	no amplification product
8	138/138
9	133/111
10	no amplification product

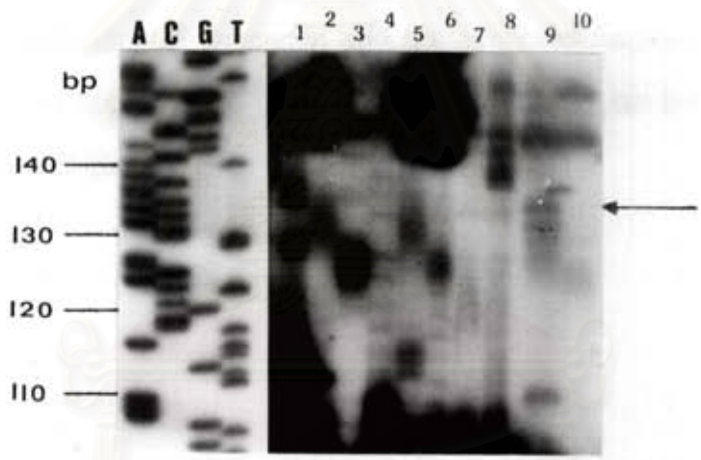

Figure 3.22 PCR amplification patterns of Pmo 519 locus from 10 unrelated individual P. monodon DNA at 55°C annealing temperature under the standard PCR conditions. The M13 sequencing ladder was used as standard size marker. An Arrow indicated microsatellite alleles.

Pmo 524 locus

This locus contained dinucleotide repeats, $(GT)_{55}$. The nucleotide sequences of the microsatellite clone is shown by Figure 3.23. The annealing temperature for Pmo 524 locus were estimateted to 57°C and 53°C for forward and reverse primers respectively. PCR amplifications of Pmo 524 locus were initially performed at 53°C under the standard PCR conditions for both labeled primers. The results in Figure 3.24 showed nonspecific amplifications from 10 unrelated individual *P. monodon* and the expected fragments were not amplified. Although the optimization of PCR conditions were done the expected bands were still not found (data not shown).

5′

CAG GCC TCG CTA TCC TAC CTG CAC ACA TAT TTT TAT ATA CAC GTC

CGT TCA TAT ATA T $(GT)_{55}$ AAG ATA AGA CCA AAT CCA GTG GTA

3′

CCG AGC TCG ATT CGT ATC ATG TCA ATG CTG CTC TGT GTG AAT GTA

Figure 3.23 The nucleotide sequences of the microsatellite clone, Pmo524 locus and the primers designed from the flanking regions (under lined).

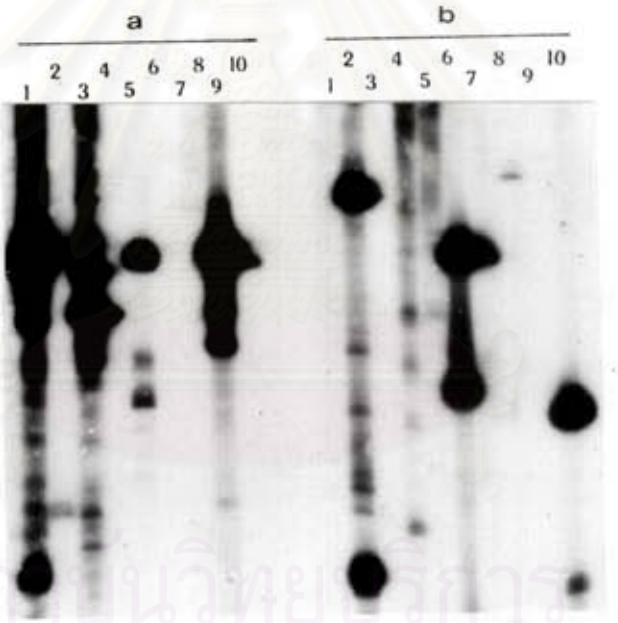

Figure 3.24 PCR amplification patterns of Pmo 524 locus from 10 unrelated individual *P. monodon* DNA at 53°C for the initial annealing temperature under the standard PCR conditions.

a. ^{32}P-labeled reward primer

b. ^{32}P-labeled forward primer